Structural Study of the Disordered *RE*Cd$_6$ Quasicrystal Approximants (*RE* = Tb, Ho, Er, Tm and Lu)

Shu Ying Piao[a], Cesar P. Gómez[b], and Sven Lidin[a]

[a] Inorganic Chemistry, Arrhenius Laboratory, Stockholm University, S-106 91 Stockholm, Sweden
[b] Sendai Institute of Multidisciplinary Research for Advanced Materials, Tohoku University, 980-8577, Sendai, Japan

Reprint requests to S. Y. Piao. Fax: +46 (0)8 152187. E-mail: sypiao@inorg.su.se

Dedicated to Professor Wolfgang Jeitschko on the occasion of his 70th birthday

The crystal structures of approximants *RE*Cd$_6$ (*RE* = Tb, Ho, Er, Tm and Lu) have been refined from single crystal X-ray diffraction data. This work is a continuation of a previous study of *M*Cd$_6$ approximants [1] in which the different types of disorder of the central Cd$_4$ tetrahedra located in the dodecahedral cavities were examined. The structures of the title compounds are all similar to GdCd$_6$ and disorder was observed in all these compounds. There is a correlation between the anisotropic displacement parameter and the unit cell dimension.

Key words: Quasicrystal Approximant, Rare Earth Cadmide

Introduction

Since Tsai *et al.* [2] and Guo *et al.* [3] reported the presence of quasicrystals in the Ca-Cd and Yb-Cd system, the compounds *RE*Cd$_6$ (*RE* = rare earth elements) (Fig. 1) as 1/1 approximants have aroused a renewed interest. The reassessment of the structure of the compound CeCd$_6$ to Ce$_6$Cd$_{37}$ [4], revealed a previously unreported order in the central tetrahedron and prompted the re-examination of the structures in the *RE*Cd$_6$ system. Pay-Gómez *et al.* [1] have extensively studied some of the *M*Cd$_6$ approximants (*M* = Pr, Nd, Sm, Eu, Gd, Dy, Yb) in the rare earth–cadmium system and found different types of disorder with the central tetrahedra located in the dodecahedral cavities. This work is a continuation and completion of that study.

Experimental Section

Syntheses

The single crystals used for the structural determination were obtained by mixing chips of rare earth metal with Cd metal (shavings from a rod of pure metal) in the molar proportions of about 1:6. The mixtures were enclosed in sealed stainless steel ampoules and heated for 48 ∼ 96 h (see Table 1). In order to obtain the desired phase in a well crystallized state, it was found effective to anneal the ampoules for a period of 48 ∼ 96 h at about 20 K below the reported
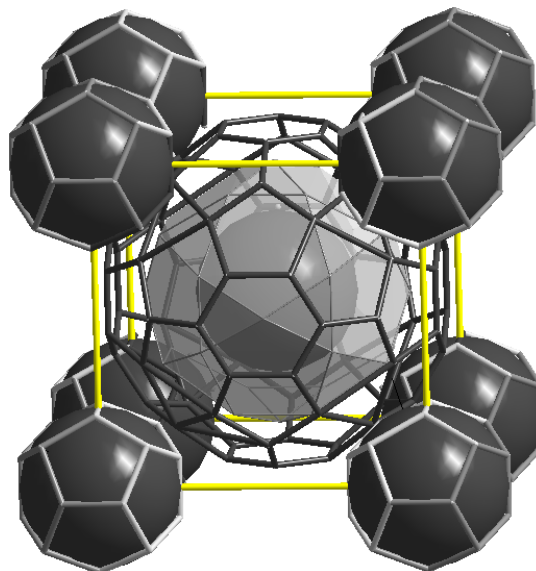

Fig. 1. The network of the *RE*Cd$_6$ phases displayed by the cluster units of Cd atoms. The dodecahedra sitting in the corner and the centre serve as cages for the disordered Cd$_4$ tetrahedra. The next shell of the dodecahedron in the centre is an icosidodecahedron, and the outermost shell in the centre is a defect triacontahedron.

melting points for each phase. For those systems where the pertinent information was lacking, several different annealing temperatures were tried to optimize the yield of the tar-

Compounds	Amount of *RE* metal [g]	Amount of Cd metal [g]	Reaction temperature [°C]	Reaction time [h]	Cooling rate [°/min]
TbCd$_6$	Tb: 0.1907	Cd: 0.8093	660	96	~ 3
HoCd$_6$	Ho: 0.1965	Cd: 0.8035	780	48	~ 3
ErCd$_6$	Er: 0.1992	Cd: 0.8033	800	48	~ 3
TmCd$_6$	Tm: 0.2188	Cd: 0.8734	800	48	~ 3
LuCd$_6$	Lu: 0.1652	Cd: 0.6368	820	72	~ 3

Table 1. Experimental details for syntheses of compounds *RE*Cd$_6$[a]. (*RE* = Tb, Ho, Er, Tm, Lu).

[a] The compounds PrCd$_6$, NdCd$_6$ and SmCd$_6$ were not synthesized as part of this investigation. The data for these compounds were taken from the previously published work [1].

Table 2. Crystal data, data collection and refinement parameters for the structures.

Formula	TbCd$_6$	HoCd$_6$	ErCd$_6$	TmCd$_6$	LuCd$_6$
Molar mass (g/mol)	833.4	839.4	841.7	843.4	849.4
Temperature of measurement (K)	293	293	293	293	293
Crystal system	cubic	cubic	cubic	cubic	cubic
Space group	$Im\bar{3}$	$Im\bar{3}$	$Im\bar{3}$	$Im\bar{3}$	$Im\bar{3}$
a Axis (Å)	15.453(4)	15.332(4)	15.399(4)	15.423(1)	15.330(4)
Cell volume (Å^3)	3690.1	3604.1	3651.5	3668.6	3602.7
Z	24	24	24	24	24
F(000)	8472	8520	8544	8568	8616
Calculated density (g/cm^3)	8.998	9.279	9.183	9.159	9.393
Absorption coefficient	31.5	33.7	34.0	33.1	37.0
Diffractometer	Stoe IPDS	Stoe IPDS	Stoe IPDS	Stoe IPDS	Stoe IPDS
Range of $2\theta(°)$	3.7 – 51.9	3.7 – 51.9	3.7 – 52.2	3.7 – 52.0	9.9 – 53.4
Radiation	Mo-K_α	Mo-K_α	Mo-K_α	Mo-K_α	Mo-K_α
Observed reflections $[I > 3\sigma]$	671	657	647	672	694
Independent reflections	670	656	549	651	598
R_{int} (obs/all)	9.41/9.41	4.58/4.58	12.36/12.60	5.55/5.56	6.20/6.31
Number of parameters	46	45	45	45	45
R_1(obs)	0.0369	0.0299	0.0252	0.0249	0.0327
wR_2 (all)	0.0661	0.0492	0.0300	0.0531	0.0366
Absorption correction	numerical, from shape	numerical, from shape	numerical, from shape	numerical, from shape	numerical, from shape
T_{min} , T_{max}	0.0170, 0.0746	0.0493, 0.1419	0.2810, 0.5050	0.2882, 0.5186	0.1664, 0.6645
$\Delta\rho_{max}, \Delta\rho_{min}$ (e/Å^3)	6.44, -3.25	2.11, -2.91	1.81, -2.08	1.85, -2.09	2.71, -7.58

get phase. The furnaces were then turned off with the samples left inside to cool down to ambient temperature (cooling rate 1 $\sim$ 3 °C/min). Single crystals could easily be isolated from the resulting samples. All preparations were carried out in an inert atmosphere (argon) in order to avoid detrimental effects from water vapor or oxygen. All pertinent details of the experiments are given in Table 1. Elemental impurity levels in the samples were below the detection limit of Energy Dispersive X-ray analysis (EDX).

Characterization and refinement

The single-crystal X-ray diffraction experiments were carried out on STOE imaging plate diffractometer with a rotating anode Mo-K_α X-ray source operated at 50 kV and 90 mA. The crystal to detector distance was 70 mm. The intensities of the reflections were integrated using the machine specific software. EDX analysis was performed in order to ascertain the elemental purity. Due to the irregular shape of the crystals, absorption correction on such a crystal by the actual measurement of the shape is inapplicable. Therefore, a numerical absorption correction, based on a shape obtained

by optimizing the equivalence for symmetry related reflections, was performed with the programs X-RED [5] and X-SHAPE [6]. All single crystal structure solutions and refinements started with the NdCd$_6$ model [1] using the program JANA2000 [7] or SHELXS-97/SHELXL-97. The structural analysis electron-density isosurfaces were generated using the program JMAP3D [8]. The images were rendered using the programs TRUESPACE, version 5.2 [9] and DIAMOND, version 2.1c [10].

Detailed crystallographic data* from the single crystal refinements are given in Table 2.

Structural Description and Discussion

The structures of the title compounds are essentially similar to the structure of other members in the

---

*Further details of the crystal structure investigation are available from the Fachinformationszentrum Karlsruhe, D-76344 Eggenstein-Leopoldshafen (Germany), on quoting the depository number CSD-415809, CSD-415810, CSD-415811, CSD-415812, CSD-415812, the name of the authors, and citation of the paper.
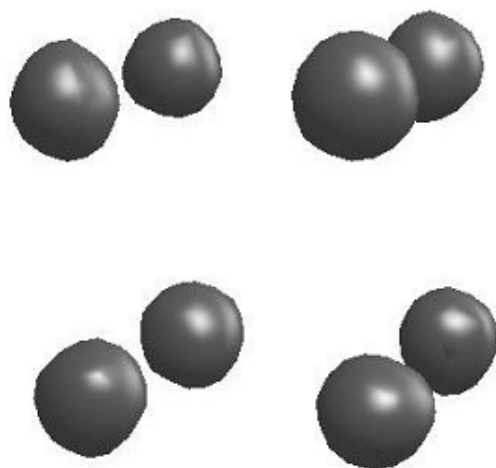
Fig. 2. Electron-density isosurfaces at the 7 e/Å^3 level for HoCd$_6$, generated from F$_{obs}$ data originating from the individual single-crystal measurements, show that there is no electron density inside the cube. None of the title compounds shows any signs of occupation of the cubes.

family as described in previous work [1]. The cluster unit of the basic building block of the RECd$_6$ phases contains 12 RECd$_{16}$ polyhedra and eight Cd$_8$ cubes. For the compounds studied previously, the innermost unit cluster (disordered tetrahedra) was described by two isotropic atomic positions, Cd1a and Cd1b, except for the case of the GdCd$_6$ phase, where the irregular shape of the atoms was modelled solely by the position Cd1a with anisotropic temperature parameters. In the present structure refinements the electron density located in the innermost cluster was modelled using a single, anisotropic atomic position. Basically the refinements reported in Table 2 are in good agreement with the result of the GdCd$_6$ case, only type II disorders [1] exist throughout all the topic compounds. The four atoms residing in the dodecahedral cavities of the title compounds form almost perfectly shaped cuboctahedra.

The additional Cd atoms occasionally located inside the Cd$_8$ cubes (*cf.* Ce$_6$Cd$_{37}$, Pr$_3$Cd$_{11-18}$ compounds) and the absence of the entire Cd$_4$ tetrahedron in one case (*cf.* Ru$_3$Be$_{17}$ [11]) are the main factors that result in the deviations from the ideal 1:6 stoichiometry of RECd$_6$ phases. But neither of these factors was observed for the title compounds. The electron-density isosurface at the 7 e/Å^3 level for HoCd$_6$ (Fig. 2) shows that there is no electron density inside the cube, and none of the title compounds shows any signs of occupation of the cubes. Thus the ideal 1:6 stoichiome-
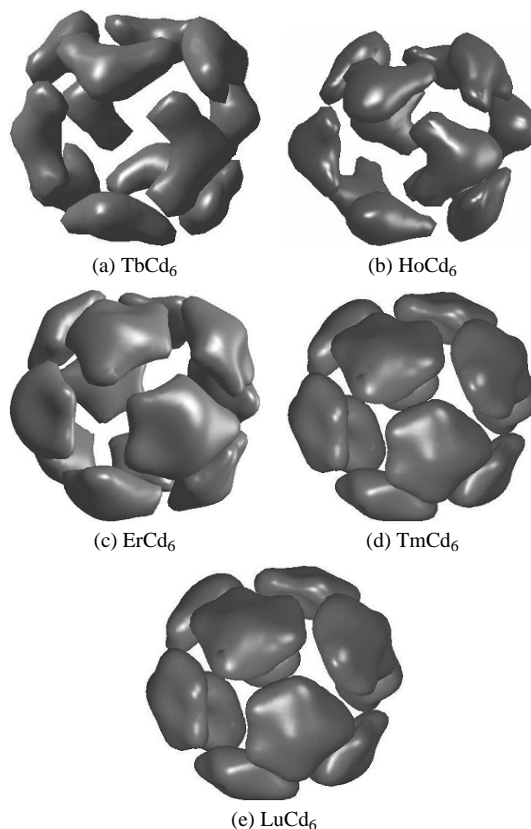

(a) TbCd$_6$ (b) HoCd$_6$

(c) ErCd$_6$ (d) TmCd$_6$

(e) LuCd$_6$

Fig. 3. Electron-density isosurfaces at the 9 e/Å^3 level, from measured electron density corresponding to the disordered tetrahedra located inside the dodecahedral cavities of the different RECd$_6$ phases, show the differences in the disorder of the Cd$_4$ tetrahedron among the title compounds.

tries of all the topic RECd$_6$ phases were maintained. This result is consistent with the hypothesis that the compounds containing an RE atom smaller than Pr are not able to accept filled cubes [12]. The electron-density isosurfaces at the 9 e/Å^3 level at the location corresponding to the centre of the dodecahedral cavity (Fig. 3) clearly show the differences in the disorder of the Cd$_4$ tetrahedron among the title compounds. In the previous report [1], the disordered tetrahedra for the phases containing Pr, Nd, Sm, and Dy were described with two atoms Cd1a and Cd1b isotropically, but it is possible to refine the positions by one anisotropic Cd1a position for the Nd, Sm and Dy compounds. For the Pr compound, this is not possible because of the complex shape of the electron density.

The atomic positions, isotropic displacement parameters and occupancies are given in Table 3. In order to correlate the disorder of the tetrahedra to the size of

M	Atom	Wyck.	Occ.	x	y	z	Ueq(Å^2)
Tb	Cd1a	24g	1/3	0	0.0827(5)	0.0763(5)	0.0950(3)
Ho	Cd1a	24g	1/3	0	0.0806(3)	0.0805(4)	0.0773(19)
Er	Cd1a	24g	1/3	0	0.0824(4)	0.0774(4)	0.080(2)
Tm	Cd1a	24g	1/3	0	0.0830(3)	0.0764(4)	0.088(2)
Lu	Cd1a	24g	1/3	0	0.0794(4)	0.0813(5)	0.0750(3)
Tb	Cd2	24g	1	0	0.09218(8)	0.24027(11)	0.0318(5)
Ho	Cd2	24g	1	0	0.09139(7)	0.23851(9)	0.0357(3)
Er	Cd2	24g	1	0	0.09203(7)	0.23958(10)	0.0315(4)
Tm	Cd2	24g	1	0	0.09219(6)	0.23985(8)	0.0297(3)
Lu	Cd2	24g	1	0	0.09106(10)	0.2382(12)	0.0394(6)
Tb	Cd4	16f	1	0.16075(6)	0.16075(6)	0.16075(6)	0.0218(3)
Ho	Cd4	16f	1	0.16039(13)	0.16050(6)	0.16050(6)	0.0203(2)
Er	Cd4	16f	1	0.16066(5)	0.16066(5)	0.16066(5)	0.0185(2)
Tm	Cd4	16f	1	0.16075(4)	0.16075(4)	0.16075(4)	0.0180(1)
Lu	Cd4	16f	1	0.16034(7)	0.16034(7)	0.16034(7)	0.0222(2)
Tb	Cd6	48h	1	0.20034(5)	0.34051(5)	0.11774(6)	0.0175(3)
Ho	Cd6	48h	1	0.19993(4)	0.34040(4)	0.11711(4)	0.0179(2)
Er	Cd6	48h	1	0.20037(5)	0.34038(5)	0.11784(5)	0.0160(2)
Tm	Cd6	48h	1	0.20039(4)	0.34041(4)	0.11801(4)	0.0147(2)
Lu	Cd6	48h	1	0.19981(6)	0.34050(6)	0.11706(6)	0.0198(3)
Tb	Cd7	12d	1	0.40574(11)	0	0	0.0291(6)
Ho	Cd7	12d	1	0.40520(8)	0	0	0.0255(4)
Er	Cd7	12d	1	0.40534(10)	0	0	0.0253(5)
Tm	Cd7	12d	1	0.40545(8)	0	0	0.0247(4)
Lu	Cd7	12d	1	0.40503(13)	0	0	0.0271(7)
Tb	Cd8	24g	1	0	0.34569(7)	0.40417(7)	0.0141(4)
Ho	Cd8	24g	1	0	0.34428(5)	0.40418(5)	0.0151(2)
Er	Cd8	24g	1	0	0.34512(6)	0.40417(6)	0.0128(3)
Tm	Cd8	24g	1	0	0.34541(5)	0.40414(5)	0.0114(2)
Lu	Cd8	24g	1	0	0.34398(8)	0.40437(8)	0.0176(4)
Tb	Cd9	12e	1	0.19033(9)	1/2	0	0.0160(5)
Ho	Cd9	12e	1	0.18827(8)	1/2	0	0.0177(3)
Er	Cd9	12e	1	0.18921(9)	1/2	0	0.0147(4)
Tm	Cd9	12e	1	0.18956(7)	1/2	0	0.0140(3)
Lu	Cd9	12e	1	0.18759(12)	1/2	0	0.0196(6)
Tb	Tb1	24g	1	0	0.29945(4)	0.18909(4)	0.0113(3)
Ho	Ho1	24g	1	0	0.29903(3)	0.18777(3)	0.0114(2)
Er	Er1	24g	1	0	0.29947(4)	0.18887(4)	0.0104(2)
Tm	Tm1	24g	1	0	0.29949(3)	0.18915(3)	0.0112(1)
Lu	Lu1	24g	1	0	0.29881(5)	0.18759(5)	0.0166(3)

Table 3. Atomic coordinates and equivalent isotropic atom displacement parameters of *RE*Cd$_6$ phases (*RE* = Tb, Ho, Er, Tm, Lu).

the rare earth element, the largest anisotropic component, U_{11}, was compared to the unit cell dimensions. In Fig. 4 the magnitude of U_{11} is represented as a function of the unit cell dimension of the *RE*Cd$_6$ phases. A well defined trend is observed, wherein the motion of the atoms making up the tetrahedron inside the dodecahedral cavity depends strongly on the size of the unit cell, and consequently on the effective size of the rare earth atoms.

Conclusion

The cluster unit of the basic building block of the title compounds is the same as for the other members in the *RE*Cd$_6$ family, built up of 12 *RE*Cd$_{16}$ polyhedra and eight Cd$_8$ cubes. The structure of the title compounds closely resembles that of GdCd$_6$. While 1:6 compounds formed with large rare earth elements show a remarkable diversity of disorders, the smaller rare earth elements lead to smaller central cavities that do not allow for such behavior. Further, none of the title compounds shows any occupancy of the Cd$_8$ cubes. It would seem that large rare earth elements tend to expand the Cd-network, leading to the creation of larger cavities; the Cd$_8$ cubes are able to host additional Cd atoms. The network formed by the Cd$_8$ cubes and the dodecahedral cavities is a strongly correlated system, and the presence of Cd atom inside the Cd$_8$ cubes results in a deformation of the dodecahedral cavity, making the environment much less spherical. Thus, for compounds with ordered cube occupancies, there is a
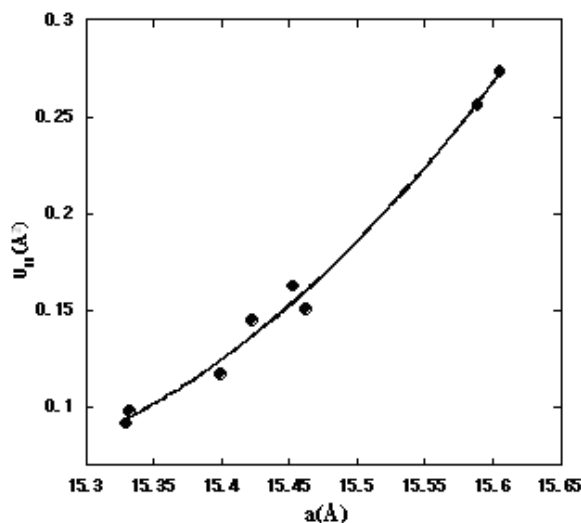
Fig. 4. The magnitude of U$_{11}$ is represented as a function of the unit cell dimension of the *RE*Cd$_6$ phases. A well defined trend shows that the motion of the atoms making up the tetrahedron inside the dodecahedral cavity depends strongly on the size of the unit cell, and consequently on the effective size of the rare earth element.

strong tendency towards oriental ordering of the central tetrahedra as well. It is the case that we see in Eu and Ce compounds (Fig. 5). As the size of the rare earth element goes down from intermediate to small sizes, the displacement ellipsoids of the Cd atoms shrink. Thus there is not enough space inside the cubes. Since there are no filled cubes, the central tetrahedron has a much more isotropic environment, and the tendency for ordering disappears. The shrinking of the dodecahedral cavity does, however, lead to a more restricted motion of the tetrahedron as it goes down in size. The decreasing free volume in the central cavity is clearly displayed in the dependence of the anisotropic displacement parameters (U$_{11}$) of the tetrahedra atoms on the unit cell dimensions. It is interesting to speculate on the behavior of the atoms in this position as the radius relation between the minority and majority atoms is decreased further, and there are reports on empty dodecahedral cavities [13], but these need further substantiation.

It is noteworthy that for the cubic structure, the size of the unit cell depends strongly on the size of the rare earth element. However a recent study on the hexagonal *RE*$_{13}$Zn$_{\sim 58}$ (*RE* = rare earth) approximants system [14] shows that the size of the unit cell changes very little with the size of the rare earth element. Further,
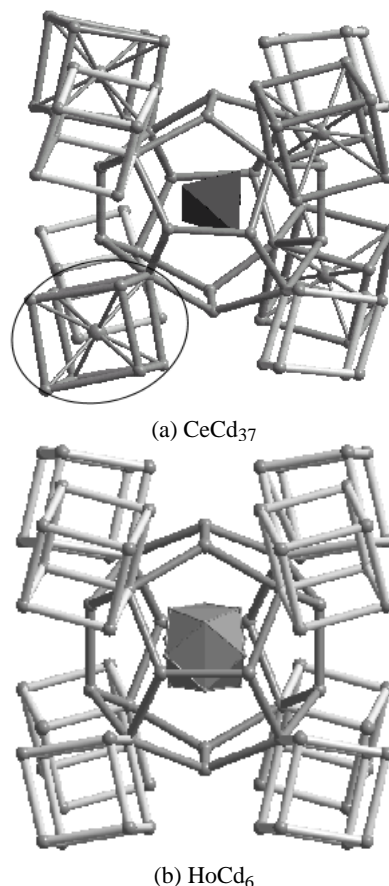

(a) CeCd$_{37}$

(b) HoCd$_6$

Fig. 5. Within the dodecahedral cavity surrounded by cubes, a Cd$_4$ unit resides. The disorder of this entity is determined by the interstitial positions in the surrounding. (a) half of the cubic interstices in Ce$_6$Cd$_{37}$ compound are filled by Cd atoms. Note how the filled cube in the circle displaces one of the vertices of the dodecahedron towards the centre. To avoid short Cd-Cd distances, all vertices of the tetrahedra are oriented towards vacant cubes and all the faces towards occupied cubes. (b) For cases when the cubes are all empty, the dodecahedron is undistorted, and as a consequence, there is no preferred orientation of the tetrahedron.

for the hexagonal systems, the concentration of interstitial Zn increases with decreasing rare earth element size, a clear reversal of the trend from the cubic systems. This may be understood in terms of the size determining species in the two cases; for the cubic system, the unit cell size is determined by the rare earth element, and hence larger rare earth elements lead to larger cavities. In the hexagonal systems the unit cell size is instead determined by the Zn-network, and hence, smaller rare earth element leads to an increase in space for interstitial atoms.

[1] C. P. Gómez, S. Lidin, Phys. Rev. B **68**, 024203 (2003).

[2] A. P. Tsai, J. Q. Guo, E. Abe, H. Takakura, T. J. Sato, Nature **408**, 537 (2000).

[3] J. Q. Guo, E. Abe, A. P. Tsai, J. Phys. Rev. B **62**, R14605 (2000).

[4] M. Armbrüster, S. Lidin, J. Alloys Comp. **307**, 141 (2000).

[5] Computer code X-RED, version 1.07, Stoe and Cie GmbH, Darmstadt, Germany (1996).

[6] X-SHAPE, Crystal optimization for numerical absorption correction, version 1.01 (Stoe and Cie GmbH, Darmstadt, Germany), (1996).

[7] V. Petříček, M. Dusek, computer code JANA2000, Institute of Physics AVCR, Praha, Czech Republic (2002).

[8] S. Weber, computer code JMAP3D (NIRIM, Tsukuba, Japan (1999).

[9] R. Ormandy, computer code TRUESPACE, version 5.2, Caligari Corporation, Mountain View, USA (2000).

[10] K. Brandenburg, computer code DIAMOND, version 2.1c, Crystal Impact, Bonn, Germany (1999).

[11] T. B. Massalski, Binary Alloy Phase Diagrams, 2nd ed., American Society for Metals, Metals Park, OH (1996).

[12] C. P. Gómez, thesis, Stockholm University (2003).

[13] D. E. Sands, Q. C. Johnson, O. H. Kikorian, K. L. Kromholtz, Acta Crystallogr. **15**, 1191 (1962).

[14] S. Y. Piao, C. P. Gómez, S. Lidin, Zeitschrift Kristallograph. (2005), in press.